IEEE Photonics Journal
An IEEE Photonics Society Publication

Open Access

Tunable and Broadband Microwave Frequency Comb Generation Using Optically Injected Semiconductor Laser Nonlinear Dynamics

Volume 9, Number 5, October 2017

Yue-Nan Li
Li Fan
Guang-Qiong Xia
Zheng-Mao Wu

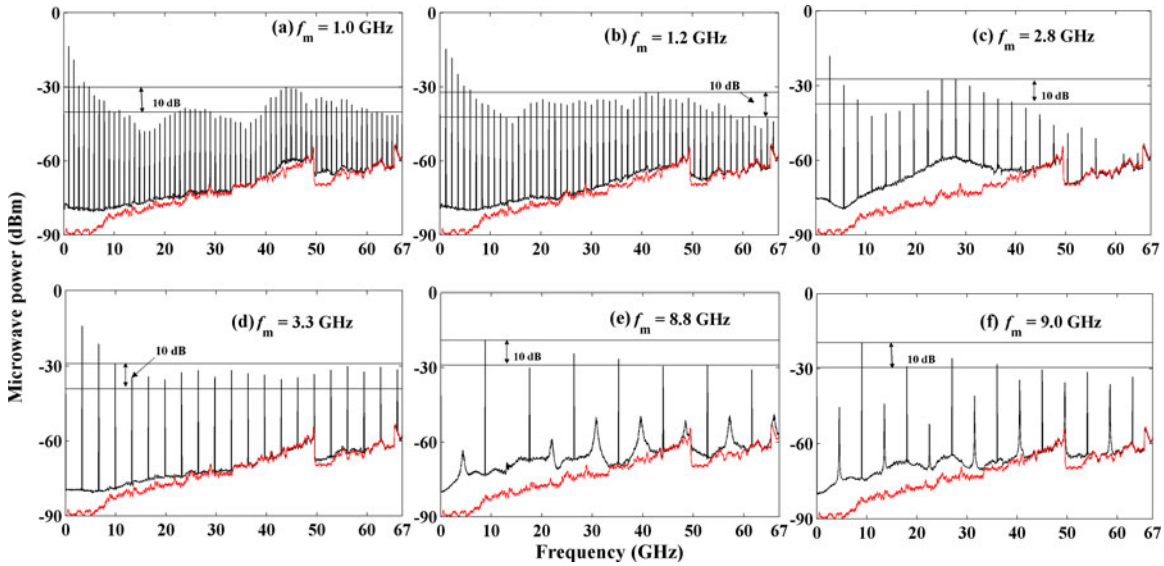

DOI: 10.1109/JPHOT.2017.2727525
1943-0655 © 2017 IEEE

Tunable and Broadband Microwave Frequency Comb Generation Using Optically Injected Semiconductor Laser Nonlinear Dynamics

Yue-Nan Li,[1] Li Fan,[1,2] Guang-Qiong Xia,[1] and Zheng-Mao Wu[1]

[1]School of Physical Science and Technology, Southwest University, Chongqing 400715, China
[2]School of Electronic and Information Engineering, Southwest University Chongqing 400715, China

DOI:10.1109/JPHOT.2017.2727525

Manuscript received May 12, 2017; revised July 12, 2017; accepted July 12, 2017. Date of publication July 17, 2017; date of current version July 27, 2017. This work was supported in part by the National Natural Science Foundation of China under Grants 61475127, 61575163, and 61640004, in part by the Natural Science Foundation of Chongqing City under Grant CSTC2016jcyjA0575, and in part by the Fundamental Research Funds for the Central Universities of China under Grant XDJK2017B047. Corresponding authors: Guang-Qiong Xia and Zheng-Mao Wu (e-mail: gqxia@swu.edu.cn; zmwu@swu.edu.cn).

Abstract: Based on an optically injected semiconductor laser (OISL) operating at period-one (P1) nonlinear dynamical state, tunable and ultrabroadband microwave frequency combs (MFCs) are generated experimentally through further current-modulating the OISL. First, by introducing an injection light with an injection power of $P_i = 12.42$ mW, whose wavelength is identical to the central wavelength of a free-running distributed feedback semiconductor laser, the OISL can be driven into P1 state with a fundamental frequency of $f_0 = 26.44$ GHz. Next, further modulating the OISL with a modulation frequency of $f_m = 3.3$ GHz and a modulation power of $P_m = 22.0$ dBm, an MFC with a bandwidth of 59.4 GHz within a 10 dB amplitude variation is experimentally obtained, and the single sideband phase noise at offset frequency 10 kHz for all comb lines contained within the bandwidth is below -95.0 dBc/Hz. Finally, through varying the modulation frequency, the MFCs with different comb spacing can be obtained, and the influences of relevant operation parameters on the performances of the generated MFCs have been analyzed.

Index Terms: Semiconductor laser, optical injection, microwave frequency combs.

1. Introduction

Nonlinear dynamics of semiconductor lasers (SLs) have been studied extensively in the past few decades. Under different perturbations such as optical injection [1]–[3], optical feedback [4]–[6], and optoelectronic feedback [7], [8], various nonlinear dynamical states including period, multiple-period, chaos, frequency locking, regular pulsing, quasi-period pulsing, chaotic pulsing have been observed [9]–[14], which can be applied in optical chaotic communication [15]–[18], sensors [19], all-optical frequency conversion [20], radio-over-fiber (RoF) transmission [21]–[25] *etc*. In particular, various approaches such as short-cavity distributed reflector laser [23], compact electro-absorption modulator integrated with vertical-cavity surface-emitting lasers (VCSELs) [24], and transverse-coupled-cavity VCSELs [25] have been proposed to meet the requirements of high speed and

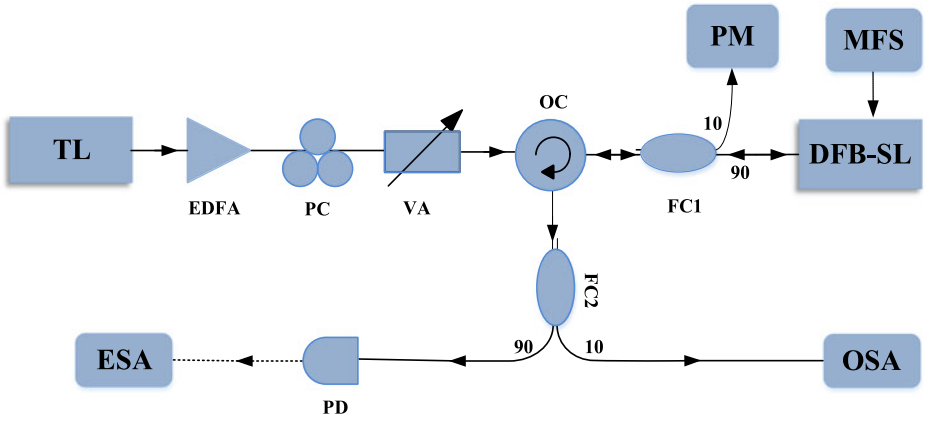

Fig. 1. Experimental setup for MFC generation. TL: tunable laser; DFB-SL: distributed feedback semiconductor; EDFA: erbium doped fiber amplifier; PC: polarization controller; VA: variable attenuator; OC: optical circulator; FC: fiber coupler; PD: photodetector; OSA: optical spectrum analyzer; ESA: electrical spectrum analyzer; PM: power meter; MFS: microwave frequency synthesizer. Solid line: optical path; dash line: electric path.

efficient modulation in the millimeter wave range for RoF applications. Remarkably, the application of the nonlinear dynamics in SLs has been extended into the generations of microwave signals [26]–[33] and microwave frequency combs (MFCs) [34]–[36]. For the MFC generation, a scheme based on harmonic frequency-locked states in a negative optoelectronic feedback (NOEF) laser is proposed and investigated [34], and the generated MFC has a bandwidth (BW) of a few GHz due to the limitation of electronic BW in the feedback loop. Based on a SL subject to optical pulse injection from an optoelectronic feedback laser, another scheme for generating MFC is also presented, and the BW of generated MFC can reach 20 GHz within a $\pm$5 dB amplitude variation [35], [36]. However, limited by electronic BW of optoelectronic feedback loop, it is very difficult to obtain broadband MFC with BW more than 40 GHz since the line spacing of MFC is determined by the repetition frequency of injected optical pulse, and thus the line spacing of MFC can only be tuned within a small range through adjusting the feedback parameters to change the repetition frequency of the injection pulse.

In this work, a novel scheme based on an optically injected semiconductor laser (OISL) is presented and experimentally demonstrated to generate MFC. Different from [35], [36], in this scheme, a continuous wave (CW) light output from a tunable laser (TL) is used as injection light to drive a distributed feedback semiconductor laser (DFB-SL) into period one (P1) oscillation with a frequency higher than the relaxation oscillation frequency of the DFB-SL. Through further introducing current modulation, broadband MFCs can be obtained under suitable operation parameters. Since the comb spacing is solely depended on the modulation frequency, the line spacing of generated MFC is relatively easy to control and can be tuned in a wide range.

2. Experimental Setup

Fig. 1 shows the experimental setup of MFC generation system. Such a system is based on a 1550 nm single-mode DFB-SL subjected to an optical injection from a tunable laser (TL, Santec TSL-710) with a wide tuning range of 1480 nm–1640 nm. The bias current and temperature of the DFB-SL are controlled by a high accuracy and low noise current-temperature controller (ILX-Lightwave LDC-3724B). The measured threshold current of the DFB-SL is $I_{th} = 4.00$ mA. Throughout the experiment, the temperature and the bias current of the DFB-SL is stabilized at 20.17 °C and 25.00 mA, respectively. Under this bias level, the free-running DFB-SL oscillates at a peak wavelength of about 1549.03 nm with a relaxation oscillation frequency f_r of about 8.66 GHz. The TL output is injected into the DFB-SL through a erbium doped fiber amplifier (EDFA), a polarization controller (PC), a variable attenuator (VA), an optical circulator (OC) and a fiber coupler (FC1)

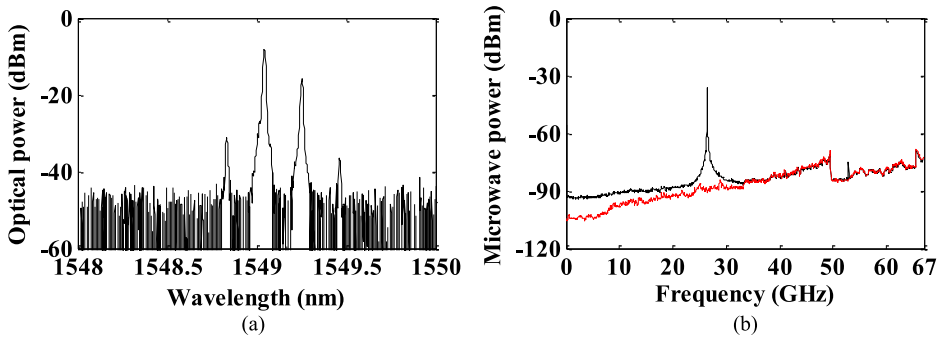

Fig. 2. Optical spectrum (a) and power spectrum (b) of the OISL under an injection power of P_i = 12.42 mW. The red line upon power spectrum denotes the noise floor.

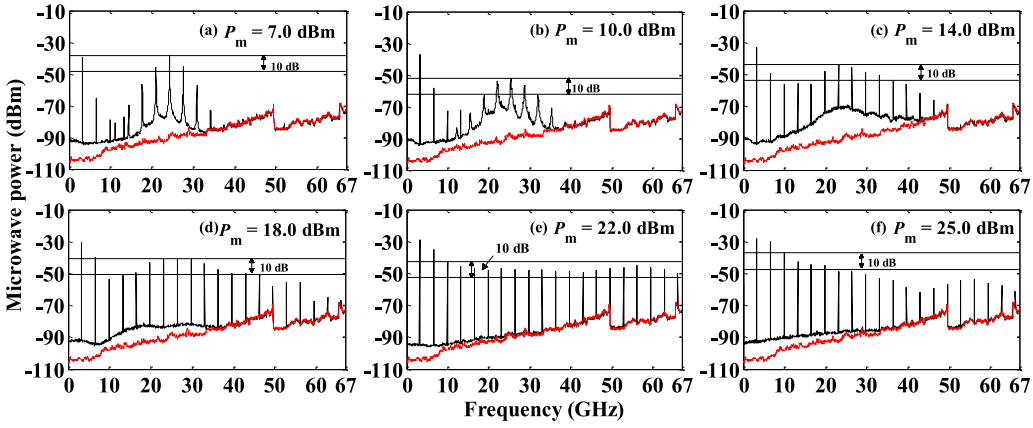

Fig. 3. Power spectra output from the OISL with f_m = 3.3 GHz and different modulation powers. The red lines upon power spectra denote the noise floor, and RBW of the ESA is set at 100 kHz.

to drive the DFB-SL into P1 oscillation. PC is employed to match the polarization state between TL and DFB-SL, and VA is used to adjust injection power. The injection power can be estimated through measuring the power at the other output port of FC1. Microwave signal generated by a microwave frequency synthesizer (MFS) is used to directly current-modulate the OISL, and the tunability of MFC can be realized through simply varying the modulation frequency (f_m). The output signals of such system are detected by an optical spectrum analyzer (OSA, Ando AQ6317C) and a 67 GHz power spectrum analyzer (ESA, Rohde & Schwarz-FSW) via a 70 GHz photodetectors (PD, U2T-XPDV3120R). In this work, the wavelength of injection light is set at the peak wavelength of free-running DFB-SL.

3. Experimental Results and Discussion

Fig. 2 displays the optical spectrum and power spectrum of the DFB-SL subject to an optical injection with an injection power of P_i = 12.42 mW. From this diagram, one can see that multiple peaks with the same spacing emerge upon the optical spectrum [see Fig. 2(a)], and the beats among multiple optical components result in P1 oscillation with a fundamental frequency of f_0 = 26.44 GHz [see Fig. 2(b)], which is about three times of the relaxation oscillation frequency of free-running DFB-SL. Meanwhile, very weak second-order harmonic at 2 f_0 can also be observed.

MFC can be generated through further introducing current modulation into the OISL. Fig. 3 shows the power spectra output from the OISL under current modulations with f_m = 3.3 GHz and different

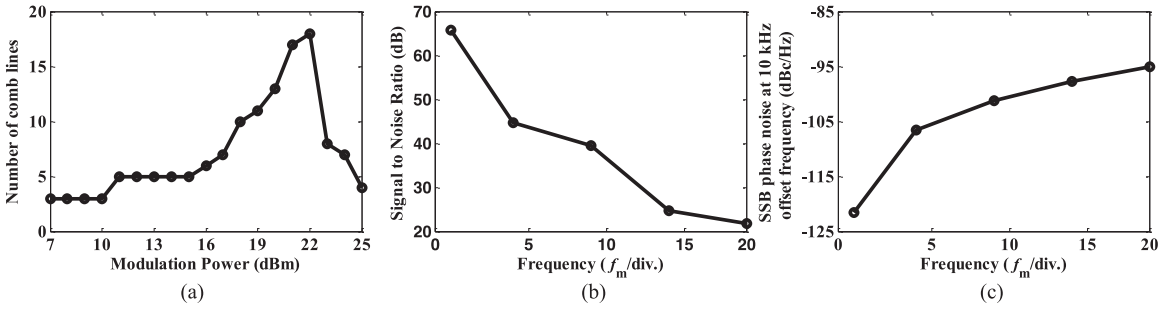

Fig. 4. (a) Dependence of the number of comb lines contained within the bandwidth on the modulation power P_m for $f_m = 3.3$ GHz, (b) SNR and (c) SSB phase noise at 10 kHz offset frequency of some representative comb lines for $f_m = 3.3$ GHz and $P_m = 22.0$ dBm.

modulation power P_m. As shown in this diagram, due to current modulation, the highest comb line is the one whose frequency is equal to f_m meanwhile the first few comb lines located at low frequencies are much greater than the other high-order harmonics. Therefore, for convenience the comb lines located at frequencies below 7.0 GHz are excluded for analyzing the BW of MFC. In this work, the BW of MFC is defined as, after excluding 0–7 GHz, the continuous frequency range within which the power differences among the comb lines are not less than 10 dB. Certainly, the BW of MFC can also be characterized by the number (n) of comb lines contained within the frequency BW, and then the BW is equal to $(n-1)f_m$. For P_m is relatively small [see Fig. 3(a) and (b)], the comb lines only exist at these locations whose frequencies are lower than or near to f_0, the power spectra are uneven and there is a valley at about 9.9 GHz. Generally, under solely current modulation, the powers of the comb lines will decrease with the increase of the harmonic order. However, the relaxation oscillation of DFB-SL and the P1 oscillation lead to enhancements at near to f_r and f_0. For $f_m = 3.3$ GHz, the enhanced effect of the laser relaxation oscillation is relatively weak, and the enhanced action mainly comes from the P1 oscillation. For the comb line with a frequency of 9.9 GHz, which is 3 times of f_m, the enhanced effect supported by P1 is low, and then a valley is formed at 9.9 GHz. Certainly, for other operating parameters, the valley location may move to some another frequency. The strongest comb line above 7.0 GHz is near to f_0, only 3 comb lines are observed within 10 dB amplitude variation, and the corresponding bandwidths are 6.6 GHz. For P_m is increased to 14.0 dBm, more harmonic components appear upon the spectrum [see Fig. 3(c)]. Further increasing P_m [see Fig. 3(d) and (e)], higher-order comb lines are observed and their powers increase with the increase of P_m. For $P_m = 22.0$ dBm [see Fig. 3(e)], the generated MFC has a bandwidth of 59.4 GHz within 10 dB amplitude variation and there are 18 comb lines contained within the BW, and the power at 9.9 GHz is obviously enhanced due to relatively strong P_m. Meanwhile, the obtained MFC possesses very little frequency drift due to the locking effect caused by the relatively strong modulation with $P_m = 22.0$ dBm, and the MFC can maintain stable for tens of minutes. It should be noted that the harmonics beyond 67 GHz cannot be observed due to the BW limitation of used ESA. As for more strong P_m [see Fig. 3(f)], the flatness of power spectrum worsens, which results in the decrease of the MFC BW. Therefore, in order to generate wide BW MFC, P_m should be taken suitable value. Additionally, above results are obtained for the temperature of DFB-SL is stabilized at 20.17 °C. When the laser temperature is set at other values, the P1 frequency f_0 will be changed, which may result in power distribution variation of comb lines. As a result, other matched values of P_m need to be selected for generating wide BW MFC.

Fig. 4(a) depicts the dependence of the number of comb lines contained within the BW on the modulation power under $f_m = 3.3$ GHz. With the increase of P_m, the number of comb lines contained within the MFC BW increases gradually, after arrives at its maximum, and then rapidly decreases. The optimum lines of comb emerge at $P_m = 22$ dBm. In this scheme, the current modulation leads to a decreased tendency of the comb lines powers with the increase of the harmonic order, and the laser relaxation oscillation and P1 oscillation result in resonantly enhancements for the comb

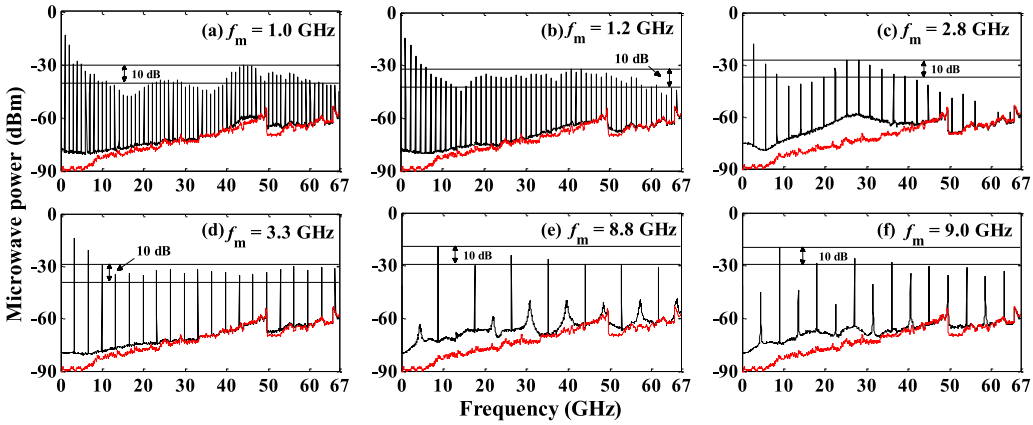

Fig. 5. Power spectra of the OISL under $P_m = 22.0$ dBm and different modulation frequency. The red lines upon power spectra denote the noise floor, and RBW of the ESA is set at 100 kHz.

lines with frequencies near to f_r or f_0. As a result, the power distribution of comb lines is determined by joint actions of the three factors mentioned above. Under such given operation condition, the power fluctuation arrives at minimum under $P_m = 22$ dBm [as shown in Fig. 3(e)], and therefore the optimum lines of comb are obtained. Furthermore, the performances of the comb lines have been examined through measuring the signal to noise ratio (SNR) and single-sideband (SSB) phase noise at 10 kHz offset frequency for some representative comb lines, which are given in Fig. 4(b) and (c), respectively. As shown in Fig. 4(b) and (c), with the increase of the order of the harmonic, SNR decreases and SSB phase noise increases. Even so, for all comb lines, it can be guaranteed that the SNRs are larger than 20 dB and the SSB phase noises are lower than -95.0 dBc/Hz.

Above results are obtained under a given f_m and varied P_m. In the following, we will fix the modulation power at 22.0 dBm and discuss the influence of the modulation frequency f_m. Fig. 5 shows the power spectra of the OISL under $P_m = 22.0$ dBm and different f_m. From this diagram, it can be seen that, under the fixed P_m level, the distribution of power spectra is varied with f_m. For $f_m = 1.0$ GHz [see Fig. 5(a)], after excluding the comb lines bellow 7.0 GHz, the strongest power comb line locates at 44.0 GHz, and there are 21 comb lines within the BW. For $f_m = 1.2$ GHz [see Fig. 5(b)], an obvious valley is observed at about 14.4 GHz, and the generated MFC has a BW of 42.0 GHz and 36 comb lines within the BW. For $f_m = 2.8$ GHz [see Fig. 5(c)], the comb lines with frequencies near f_0 possess relatively strong powers, and the powers of comb lines decrease quickly once the frequencies of comb lines are deviated from f_0, which results in a relatively small BW. However, for $f_m = 3.3$ GHz [see Fig. 5(d)], the power spectrum becomes flat except that the amplitudes of the first and second comb lines are 10 dB larger than those of the others. As a result, the generated MFC has a 59.4 GHz BW and 18 comb lines contained within the BW. For relatively large values of $f_m = 8.8$ GHz and 9.0 GHz [see Fig. 5(e) and (f)], some new frequency components with frequencies of $nf_m/2$ are observed, and the frequency spacing is no longer f_m, which are beyond the scope of this work. Therefore, in the following discussion, we only analyze the case that f_m is no more than 8.0 GHz.

Finally, the variations of the BW and the number of comb lines contained within the BW with the modulation frequency are shown in Fig. 6 under $P_m = 22.0$ dBm. For comparison, the case for directly modulated DFB-SL without optical injection has also been shown. On the whole, the bandwidth and the number of comb lines can be enhanced after introducing optical injection. The maximum of the BW (59.4 GHz) emerges at $f_m = 3.3$ GHz, and the most comb lines (36 comb lines) is obtained for $f_m = 1.2$ GHz. It should be noted that the BW and the number of comb lines of the MFCs generated by OISL are relatively small for 2.0 GHz $\leq f_m \leq$ 3.2 GHz, which is due to uneven power spectrum and the BW definition used in this work.

It should be pointed out that, although above results are obtained under the case that the peak wavelength of injection light is set at the peak wavelength of free-running DFB-SL, further

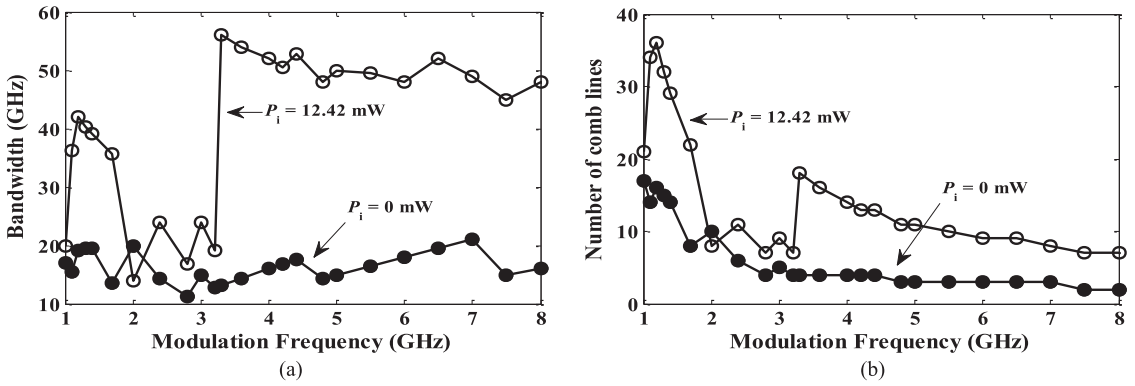

Fig. 6. Variations of the BW (a) and the number of comb lines (b) of MFCs with modulation frequency under $P_m = 22.0$ dBm for $P_i = 0$ mW and $P_i = 12.42$ mW, respectively.

preliminarily experimental results demonstrate that high-quality MFCs can also be generated if the wavelength of injection light has a small deviation from the peak wavelength of free-running DFB-SL.

4. Conclusion

In conclusion, a novel scheme for generating tunable and broadband microwave frequency comb (MFC) is proposed, and the performances of generated MFC are analyzed. In this scheme, an optically injected 1550 nm DFB-SL operating at period-one (P1) nonlinear dynamical state is used as a seed source for the MFC generation. For the injection light with injection power of $P_i = 12.42$ mW and the same wavelength as that of the free-running DFB-SL, the optically injected semiconductor laser (OISL) is driven into P1 dynamical state with a fundamental frequency of $f_0 = 26.44$ GHz. Further directly current-modulating the OISL, tunable and broadband MFCs can be obtained through selecting suitable modulation parameters. The experimental results show that, for a given modulation frequency $f_m = 3.3$ GHz, the bandwidth of MFC is influenced by the modulation power P_m. For $P_m = 22.0$ dBm, the bandwidth of generated MFC arrives at the maximum of 59.4 GHz within a 10 dB amplitude variation, and the single sideband (SSB) phase noise at offset frequency 10 kHz for all comb lines contained within the bandwidth are below -95.0 dBc/Hz. For a given modulation power $P_m = 22.0$ dBm, the MFCs with different comb spacing can be obtained through adjusting the modulation frequency f_m.

References

[1] T. B. Simpson, J. M. Liu, K. F. Huang, and K. Tai, "Nonlinear dynamics induced by external optical injection in semiconductor lasers," *Quantum Semiclassical Opt.*, vol. 9, no. 5, pp. 765–784, May 1997.
[2] S. Wieczorek, B. Krauskopf, and D. Lenstra, "Multipulse excitability in a semiconductor laser with optical injection," *Phys. Rev. Lett.*, vol. 88, no. 6, Jan. 2002, Art. no. 063901.
[3] S. Eriksson and Å. M. Lindberg, "Observations on the dynamics of semiconductor lasers subjected to external optical injection," *J. Opt. B: Quantum Semiclassical Opt.*, vol. 4, no. 2, pp. 149–154, Mar. 2002.
[4] T. Heil, I. Fischer, and W. Elsäßer, "Dynamics of semiconductor lasers subject to delayed optical feedback: the short cavity regime," *Phys. Rev. Lett.*, vol. 87, no. 24, Nov. 2001, Art. no. 243901.
[5] R. Ju and P. S. Spencer, "Dynamic regimes in semiconductor lasers subject to incoherent optical feedback," *J. Lightw. Technol.*, vol. 23, no. 8, pp. 2513–2523, Aug. 2005.
[6] A. Hohl and A. Gavrielides, "Bifurcation cascade in a semiconductor laser subject to optical feedback," *Phys. Rev. Lett.*, vol. 82, no. 6, pp. 1148–1151, Feb. 1999.
[7] C. H. Lee and S. Y. Shin, "Self-pulsing, spectral bistability, and chaos in a semiconductor laser diode with optoelectronic feedback," *Appl. Phys. Lett.*, vol. 62, no. 9, pp. 922–924, Mar. 1993.
[8] F. Y. Lin and J. M. Liu, "Nonlinear dynamics of a semiconductor laser with delayed negative optoelectronic feedback," *IEEE J. Quantum Electron.*, vol. 39, no. 4, pp. 562–568, Apr. 2003.

[9] L. X. Zou *et al.*, "Nonlinear dynamics for semiconductor microdisk laser subject to optical injection," *IEEE J. Sel. Topics Quantum Electron.*, vol. 21, no. 6, Nov./Dec. 2015, Art. no. 1800408.
[10] A. Gavrielides, V. Kovanis, M. Nizette, T. Erneux, and T. B. Simpson, "Period three limit-cycles in injected semiconductor lasers," *J. Opt. B: Quantum Semiclassical Opt.*, vol. 4, no. 1, pp. 20–26, Jan. 2002.
[11] F. Y. Lin and J. M. Liu, "Harmonic frequency locking in a semiconductor laser with delayed negative optoelectronic feedback," *Appl. Phys. Lett.*, vol. 81, no. 17, pp. 3128–3130, Oct. 2002.
[12] J. Mork, B. Tromborg, and J. Mark, "Chaos in semiconductor lasers with optical feedback: theory and experiment," *IEEE J. Quantum Electron.*, vol. 28, no. 1, pp. 93–108, Jan. 1992.
[13] B. Haegeman, K. Engelborghs, and D. Roose, "Stability and rupture of bifurcation bridges in semiconductor lasers subject to optical feedback," *Phys. Rev. E: Statist. Nonlinear Soft Matter Phys.*, vol. 66, no. 4, Oct. 2002, Art. no. 046216.
[14] F. Y. Lin, S. Y. Tu, C. C. Huang, and S. M. Chang, "Nonlinear dynamics of semiconductor lasers under repetitive optical pulse injection," *IEEE J. Sel. Topics Quantum Electron.*, vol. 15, no. 3, pp. 604–611, May/Jun. 2009.
[15] A. Argyris *et al.*, "Chaos-based communications at high bit rates using commercial fibre-optic links," *Nature*, vol. 438, no. 17, pp. 343–346, Nov. 2005.
[16] J. G. Wu, Z. M. Wu, X. Tang, L. Fan, W. Deng, and G. Q. Xia, "Experimental demonstration of LD-based bidirectional fiber-optic chaos communication," *IEEE Photon. Technol. Lett.*, vol. 25, no. 6, pp. 587–590, Mar. 2013.
[17] T. Deng, G. Q. Xia, L. P. Cao, J. G. Chen, X. D. Lin, and Z. M. Wu, "Bidirectional chaos synchronization and communication in semiconductor lasers with optoelectronic feedback," *Opt. Commun.*, vol. 282, no. 11, pp. 2243–2249, Feb. 2009.
[18] M. W. Lee, P. Rees, K. A. Shore, S. Ortin, L. Pesquera, and A. Valle, "Dynamical characterisation of laser diode subject to double optical feedback for chaotic optical communications," *IEE Proc. Optoelectron.*, vol. 152, no. 2, pp. 97–102, Apr. 2005.
[19] W. W. Chow and S. Wieczorek, "Using chaos for remote sensing of laser radiation," *Opt. Exp.*, vol. 17, no. 9, pp. 7491–7504, Apr. 2009.
[20] S. K. Hwang, H. F. Chen, and C. Y. Lin, "All-optical frequency conversion using nonlinear dynamics of semiconductor lasers," *Opt. Lett.*, vol. 34, no. 6, pp. 812–814, Aug. 2009.
[21] M. J. Zhang, Y. N. Ji, Y. N. Zhang, Y. Wu, H. Xu, and W. P. Xu, "Remote radar based on chaos generation and Radio Over Fiber," *IEEE Photon. J.*, vol. 6, no. 5, Oct. 2014, Art. no. 7902412.
[22] C. C. Cui and S. C. Chan, "Performance analysis on using period-one oscillation of optically injected semiconductor lasers for radio-over-fiber uplinks," *IEEE J. Quantum Electron.*, vol. 48, no. 4, pp. 490–499, Apr. 2012.
[23] Y. Matsui *et al.*, "55 GHz bandwidth distributed reflector laser," *J. Lightw. Technol.*, vol. 35, no. 3, pp. 397–403, Feb. 2017.
[24] H. Dalir, M. Ahmed, A. Bakry, and F. Koyama, "Compact electro-absorption modulator integrated with vertical-cavity surface-emitting laser for highly efficient millimeter-wave modulation," *IEEE Photon. Technol. Lett.*, vol. 105, no. 8, Aug. 2014, Art. no. 081113.
[25] H. Dalir, A. Matsutani, M. Ahmed, A. Bakry, and F. Koyama, "High frequency modulation of transverse-coupled-cavity VCSELs for radio over fiber applications," *IEEE Photon. Technol. Lett.*, vol. 26, no. 3, pp. 281–284, Feb. 2014.
[26] S. Y. Juan and F. Y. Lin, "Photonic generation of broadly tunable microwave signals utilizing a dual-beam optically injected semiconductor laser," *IEEE Photon. J.*, vol. 3, no. 4, pp. 644–650, Aug. 2011.
[27] J. W. Wu, Q. Qiu, X. P. Zhang, and Y. H. Won, "Simultaneous generation of microwave, millimeter-wave, and Terahertz photonic signal based on two-color semiconductor laser subject to single beam optical injection," *IEEE J. Sel. Topics Quantum Electron.*, vol. 23, no. 4, Jul./Aug. 2017, Art. no. 1800108.
[28] X. W. Ma *et al.*, "Narrow-linewidth microwave generation using AlGaInAs/InP microdisk lasers subject to optical injection and optoelectronic feedback," *Opt. Exp.*, vol. 23, no. 16, Jul. 2015, Art. no. 241717.
[29] J. P. Zhuang and S. C. Chan, "Tunable photonic microwave generation using optically injected semiconductor laser dynamics with optical feedback stabilization," *Opt. Lett.*, vol. 38, no. 3, pp. 344–346, Feb. 2013.
[30] K. H. Lo, S. K. Hwang, and S. Donati, "Optical feedback stabilization of photonic microwave generation using period-one nonlinear dynamics of semiconductor lasers," *Opt. Exp.*, vol. 22, no. 15, pp. 18648–18661, Jul. 2014.
[31] Y. H. Hung and S. K. Hwang, "Photonic microwave stabilization for period-one nonlinear dynamics of semiconductor lasers using optical modulation sideband injection locking," *Opt. Exp.*, vol. 23, no. 5, pp. 6520–6532, Mar. 2015.
[32] L. Fan, G. Q. Xia, J. J. Chen, X. Tang, Q. Liang, and Z. M. Wu, "High-purity 60 GHz band millimeter-wave generation based on optically injected semiconductor laser under subharmonic microwave modulation," *Opt. Exp.*, vol. 24, no. 16, pp. 18252–18265, Aug. 2016.
[33] A. Hurtado, I. D. Henning, M. J. Adams, and L. F. Lester, "Generation of tunable millimeter-wave and THz signals with an optically injected quantum dot distributed feedback laser," *IEEE Photon. J.*, vol. 5, no. 4, Aug. 2013, Art. no. 5900107.
[34] S. C. Chan, G. Q. Xia, and J. M. Liu, "Optical generation of a precise microwave frequency comb by harmonic frequency locking," *Opt. Lett.*, vol. 32, no. 13, pp. 1917–1919, Jul. 2007.
[35] Y. S. Juan and F. Y. Lin, "Microwave-frequency-comb generation utilizing a semiconductor laser subject to optical pulse injection from an optoelectronic feedback laser," *Opt. Lett.*, vol. 34, no. 11, pp. 1636–1638, Jun. 2009.
[36] Y. S. Juan and F. Y. Lin, "Ultra broadband microwave frequency combs generated by an optical pulse-injected semiconductor laser," *Opt. Exp.*, vol. 17, no. 21, pp. 18596–18605, Oct. 2009.